PNAS RESEARCH ARTICLE | PHYSIOLOGY

The V-type H$^+$-ATPase is targeted in antidiuretic hormone control of the Malpighian "renal" tubules

Farwa Sajadi[a], María Fernanda Vergara-Martínez[a,b], and Jean-Paul V. Paluzzi[a,1]

Edited by David Denlinger, The Ohio State University, Columbus, OH; received June 14, 2023; accepted November 1, 2023

Like other insects, secretion by mosquito Malpighian tubules (MTs) is driven by the V-type H$^+$-ATPase (VA) localized in the apical membrane of principal cells. In *Aedes aegypti*, the antidiuretic neurohormone CAPA inhibits secretion by MTs stimulated by select diuretic hormones; however, the cellular effectors of this inhibitory signaling cascade remain unclear. Herein, we demonstrate that the VA inhibitor bafilomycin selectively inhibits serotonin (5HT)- and calcitonin-related diuretic hormone (DH_{31})-stimulated secretion. VA activity increases in DH_{31}-treated MTs, whereas CAPA abolishes this increase through a NOS/cGMP/PKG signaling pathway. A critical feature of VA activation involves the reversible association of the cytosolic (V_1) and membrane (V_o) complexes. Indeed, higher V_1 protein abundance was found in membrane fractions of DH_{31}-treated MTs, whereas CAPA significantly decreased V_1 abundance in membrane fractions while increasing it in cytosolic fractions. V_1 immunolocalization was observed strictly in the apical membrane of DH_{31}-treated MTs, whereas immunoreactivity was dispersed following CAPA treatment. VA complexes colocalized apically in female MTs shortly after a blood meal consistent with the peak and postpeak phases of diuresis. Comparatively, V_1 immunoreactivity in MTs was more dispersed and did not colocalize with the V_o complex in the apical membrane at 3 h post blood meal, representing a time point after the late phase of diuresis has concluded. Therefore, CAPA inhibition of MTs involves reducing VA activity and promotes complex dissociation hindering secretion. Collectively, these findings reveal a key target in hormone-mediated inhibition of MTs countering diuresis that provides a deeper understanding of this critical physiological process necessary for hydromineral balance.

proton pump | Malpighian tubule | insect renal physiology | antidiuresis | neuropeptide

Significance

The V-type H$^+$ ATPase (VA), or proton pump, provides the driving force for transepithelial ion and fluid secretion in insect Malpighian tubules (MTs). While studies have shown diuretic stimulation activates various signaling pathways, including cAMP and downstream effectors promoting increased VA activity, our understanding of antidiuretic signaling and its potential regulation of the VA remains rudimentary. Herein, we show that CAPA neuropeptide acts through the NOS/cGMP/PKG pathway to inhibit DH_{31}-stimulated VA activity, supporting the notion that the antidiuretic regulation is achieved through dissociation of the VA complexes. These results demonstrate a critical role of VA inhibition and trafficking necessary for antidiuretic signaling and advance our understanding of the complex neuroendocrine control of the MTs in this important human disease-vector mosquito.

Insect postprandial diuresis is under rigorous control by neuroendocrine factors (1) acting on the Malpighian "renal" tubules (MTs) to regulate primary urine production. In the yellow fever mosquito, *Aedes aegypti,* several diuretics have been identified that regulate urine production including serotonin (5HT), calcitonin-related diuretic hormone (DH_{31}), corticotropin-releasing factor-related diuretic hormone (DH_{44}), and leucokinin-related (LK) diuretic hormone (2–5). In female *Aedes* mosquitoes, an antidiuretic peptidergic neurohormone, CAPA, selectively inhibits DH_{31}- and 5HT-stimulated secretion of MTs (4, 6, 7). Insect CAPA neuropeptides are produced in the central nervous system and are evolutionarily related to neuromedin U in vertebrates (8). In the fruit fly, *Drosophila melanogaster*, CAPA peptides have been shown to act through a conserved nitridergic signaling pathway to stimulate diuresis by MTs (9, 10); however, a few other studies have alluded to an antidiuretic role (11, 12). In contrast, in both larval and adult *A. aegypti*, CAPA peptides inhibit fluid secretion through a signaling cascade involving the NOS/cGMP/PKG pathway (6, 7). Despite this, the antidiuretic signaling mechanism and downstream cellular targets, such as the ion channels and transporters, remain elusive.

In insect MTs, including *A. aegypti*, the bafilomycin-sensitive V-type H$^+$ ATPase (VA), also known as the proton pump, functions as an electrogenic pump allowing the transport of protons from the cytoplasm to the tubule lumen, thus generating a cell-negative membrane voltage (13, 14). This membrane voltage can then drive secondary transport processes such as the cation/H$^+$ exchanger or anion/H$^+$ cotransporter (15, 16). Originally found in vacuolar membranes of animals and plants, the VA has since been found to be essential in cell function in both invertebrates and vertebrates (17). In insects, the VA is densely located in the apical brush border membrane of tubule principal cells (13, 18), which is rich in mitochondria and endoplasmic reticula, fueling the ATP-consuming proton pump (1, 19). Previous studies have shown VA localization within the apical membrane of principal cells along the entire length of the MTs (19), but absent in stellate cells that express relatively higher levels of the P-type Na$^+$/K$^+$ ATPase (NKA) (19). Due to stronger VA immunoreactivity observed in MTs (19), and greater ATPase activity by electrophysiological assays (13, 14), the VA is categorized

Author contributions: F.S. and J.-P.V.P. designed research; F.S. and M.F.V.-M. performed research; J.-P.V.P. contributed new reagents/analytic tools; F.S. and J.-P.V.P. analyzed data; and F.S. and J.-P.V.P. wrote the paper.

The authors declare no competing interest.

This article is a PNAS Direct Submission.

[1]To whom correspondence may be addressed. Email: paluzzi@yorku.ca.

This article contains supporting information online at https://www.pnas.org/lookup/suppl/doi:10.1073/pnas.2308602120/-/DCSupplemental.

Published December 14, 2023.

as serving mainly, but not exclusively (20), stimulated transport mechanisms, whereas the NKA serves basic cell housekeeping functions when MTs are undergoing low unstimulated rates of secretion (13, 20, 21).

Stimulation of distinct diuretic hormone receptors can activate various signaling pathways, including elevation of cyclic AMP (cAMP) levels which is known to increase VA activity and assembly in insects (22). In *A. aegypti,* DH_{31}, identified as the mosquito natriuretic peptide (23), selectively activates transepithelial secretion of Na^+ in the MTs, using cAMP as a second messenger (1), and up-regulating the VA function to stimulate fluid secretion (24). Similarly, 5HT-stimulated diuresis is also thought to be mediated (at least in part) through the cAMP second messenger pathway (25), activating protein kinase A (PKA) to increase the transepithelial voltage of the basolateral membrane in tubule principal cells (1, 26). In contrast, DH_{44} has been shown to initiate diuresis via the paracellular and transcellular pathways, with higher nanomolar concentrations increasing cAMP and Ca^{2+}, influencing both paracellular and transcellular transport, and lower nanomolar concentrations acting through the paracellular pathway only, via intracellular Ca^{2+} (27). Thus, due to its predominant role in fluid secretion, the VA could be a likely target for both diuretic and antidiuretic factors.

Eukaryotic V-ATPases are a multisubunit protein composed of up to 14 different polypeptides, which form two major structural complexes. The peripheral V_1 complex (400 to 600 kDa) is invariably present in the cytoplasm and interacts with ATP, ADP, and inorganic phosphate (28). The cytosolic V_1 complex consists of eight different subunits (A to H): a globular headpiece with three alternating subunits A and B forming a hexamer with nucleotide binding sites located at their interface, a central rotor stalk with single copies of subunits D and F, and lastly, a peripheral stalk made up of subunits C, E, G, and H (28). The B subunit, shown to have high sequence similarity among several species from fungi to mammals (29, 30), is a 56-kDa polypeptide and is one of the two sites (along with subunit A) (31) in the V_1 complex that binds ATP. In contrast, the membrane-integrated V_o complex (150 to 350 kDa) mediates the transport of H^+ across the membrane (28) and is composed of at least six different subunits, which collectively function in the proton translocation pathway (13, 28). Although the proton channel of the VA can be blocked pharmacologically by the macrolide antibiotic, bafilomycin (32), there are two known intrinsic mechanisms for VA regulation: first, through oxidation of the cystine residue on the A subunit of the V_1 complex, thus preventing ATP hydrolysis; second, through reversible disassembly of the V_1 complex from the holoenzyme (13, 33). While the role and regulation of the VA by diuretic hormones in insect MTs has been studied (34–36), research examining antidiuretic signaling mechanisms involving the VA remains in its infancy.

Considering that the *A. aegypti* mosquito is recognized as a disease vector for several viruses, further investigating the regulatory mechanisms of diuresis and antidiuresis in the MTs can allow for useful insights into novel methods to control disease transmission. This study aimed to identify the cellular targets necessary for CAPA-mediated inhibition of fluid secretion by MTs stimulated by select diuretic factors in adult female *A. aegypti*. Our results provide evidence that CAPA neuropeptides inhibit fluid secretion in the mosquito by VA complex dissociation, thus hindering VA function and activity that is essential for driving rapid postprandial diuresis.

Results

Bafilomycin Inhibits DH_{31}- and 5HT-Stimulated Fluid Secretion Rate. To determine the appropriate concentration of bafilomycin to test on adult *A. aegypti* MTs, several doses were applied against DH_{31}-stimulated tubules (*SI Appendix*, Fig. S1*A*). Higher doses of bafilomycin (10^{-4} M and 10^{-5} M) resulted in significant inhibition of fluid secretion rate, with maximal inhibition leading to a fivefold decrease, observed with treatment of 10^{-5} M bafilomycin. Next, to determine whether inhibiting the VA would decrease fluid secretion rate stimulated by other diuretic hormones, including 5HT and DH_{44}, the effect of 10^{-5} M bafilomycin on adult tubules stimulated with these diuretics was tested (Fig. 1). Fluid secretion rates were measured over 30 min under control (stimulated) conditions, and then at 10-min intervals in the presence of bafilomycin. Treatment of MTs with 10^{-5} M bafilomycin against DH_{31} led to a decrease of fluid secretion over the treatment interval. Specifically, 30 min after treatment with bafilomycin, fluid secretion rate was significantly reduced by over twofold to 0.438 ± 0.041 nL min^{-1}, compared to DH_{31} alone, 0.941 ± 0.077 nL min^{-1} (Fig. 1*A*). Similar results were seen with 5HT-stimulated MTs; however, a decrease in fluid secretion was observed 30 min post-bafilomycin, with a significant inhibition 40 min after treatment (0.522 ± 0.072 nL min^{-1}, 5HT alone vs. 0.182 ± 0.045 nL min^{-1}, 5HT+ bafilomycin) (Fig. 1*B*). Distinct from DH_{31} and 5HT-stimulated tubules, DH_{44}-stimulated secretion was insensitive to bafilomycin treatment (Fig. 1*C*). To confirm whether *Aedae*CAPA-1 antidiuresis is mediated by VA inhibition, adult female MTs were treated with either DH_{31} alone or in combination with *Aedae*CAPA-1, bafilomycin, or both (Fig. 1*D*). MTs treated with either *Aedae*CAPA-1 or bafilomycin resulted in a significant inhibition of DH_{31}-stimulated secretion, and similar inhibition was observed when both *Aedae*CAPA-1 and bafilomycin were applied together with no evidence of any additive inhibitory effects (Fig. 1*D*).

***Aedae*CAPA-1 and Bafilomycin Alkalinize Secreted Fluid in DH_{31}- and 5HT-Stimulated MTs.** The VA pumps protons from the cell into the tubule lumen thus generating an electromotive potential (20, 31) and providing energy to drive the secretion of cations via Na^+/H^+ and/or K^+/H^+ antiporters (13). An indirect way to measure whether *Aedae*CAPA-1 and bafilomycin inhibit VA activity involves measuring the pH of the secreted fluid from diuretic-stimulated MTs treated with *Aedae*CAPA-1 or bafilomycin (Fig. 1 *E*–*G*). In DH_{31}-stimulated MTs treated with *Aedae*CAPA-1, there was an immediate significantly higher pH in the secreted fluid (7.479 ± 0.030) at 40 min relative to control, increasing up to 7.73 ± 0.038 at 60 min (Fig. 1*E*). Similarly, pH levels in DH_{31}-stimulated MTs treated with bafilomycin were significantly higher (7.66 ± 0.064) relative to control at 40 min, increasing up to 7.855 ± 0.074 at 60 min. Comparable to DH_{31}, addition of *Aedae*CAPA-1 or bafilomycin, significantly increased the pH of secreted fluid from 5HT-stimulated MTs to 7.75 ± 0.061 and 7.82 ± 0.083 respectively, at the 60 min mark (Fig. 1*F*). In contrast, unlike the effects observed with DH_{31}- and 5HT-stimulated MTs, *Aedae*CAPA-1 or bafilomycin did not alter the pH of the secreted fluid in DH_{44}-stimulated MTs (Fig. 1*G*). The pH increased from 7.4 to 7.9 during the 30-min DH_{44} incubation; however, pH did not change following the addition of *Aedae*CAPA-1 or bafilomycin. Separately, we conducted measurements in unstimulated tubules to verify pH in these small droplets did not drift over a time frame consistent with our above experiments. Unstimulated MTs were allowed to secrete, and the droplets were isolated and their pH was measured over the course of 60 min. Over this incubation period, no change was observed in the pH of secreted droplets from unstimulated MTs (Fig. 1*H*), upholding the notion that the alkalinization of secreted fluid observed following *Aedae*CAPA-1 (or bafilomycin) treatment of DH_{31}- and 5HT-stimulated MTs is a result of VA inhibition. Additionally, unstimulated MTs treated with either *Aedae*CAPA-1 or bafilomycin resulted in no significant

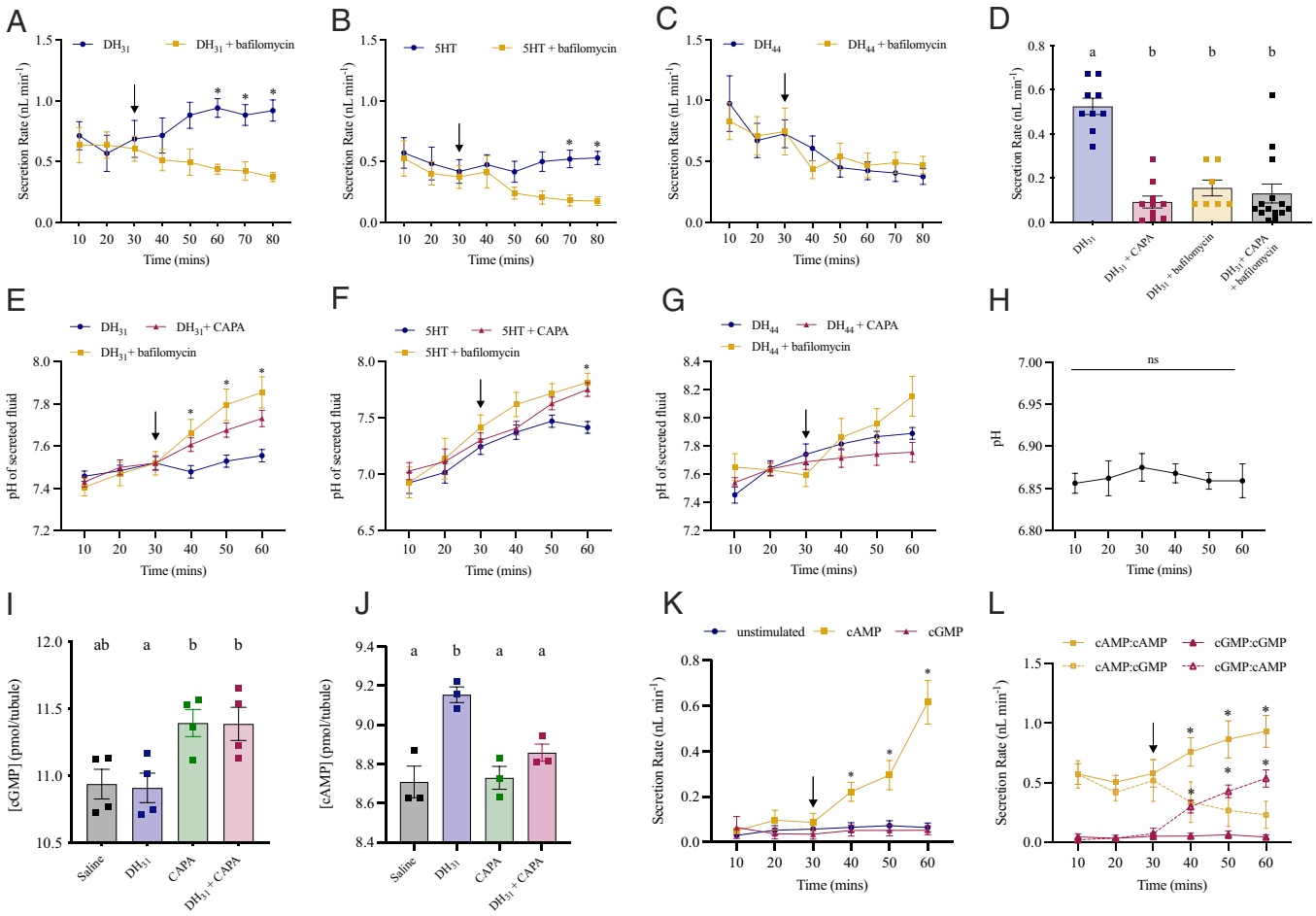

Fig. 1. Effect of bafilomycin on fluid secretion rates and pH along with cyclic nucleotide second messengers on adult *A. aegypti* MTs. Tubules were treated with either (*A*) DH_{31}, (*B*) 5HT, or (*C*) DH_{44}, and secreted droplets were measured at 10-min intervals for 30 min. Immediately following measurement of the 30-min point fluid droplet (solid arrow), MTs were treated with (*A*) DH_{31}, (*B*) 5HT, (*C*) or DH_{44} alone or in combination with *Aedae*CAPA-1 or bafilomycin. (*D*) MTs were treated with DH_{31} alone or in combination with *Aedae*CAPA-1, bafilomycin, or both *Aedae*CAPA-1 and bafilomycin for 60 min. Secreted fluid pH was measured in tubules treated with either (*E*) DH_{31} (*F*) 5HT or (*G*) DH_{44} before and after addition of *Aedae*CAPA-1 or bafilomycin, along with unstimulated MTs (*H*). Production of (*I*) cGMP and (*J*) cAMP in DH_{31}-stimulated MTs treated with *Aedae*CAPA-1. (*A–C*) Significant differences between bafilomycin-treated and the corresponding time point controls and (*E–H*) significant differences in secreted fluid pH between *Aedae*CAPA-1- and bafilomycin-treated and the corresponding time point controls are denoted by an asterisk, as determined by a two-way ANOVA and Bonferroni multiple comparison post hoc test ($P < 0.05$). Data represent the mean ± SEM (n = 12 to 34); ns denotes no statistical significance. (*D*, *I*, and *J*) Bars labeled with different letters are significantly different from each other [mean ± SEM; one-way ANOVA with Bonferroni multiple comparison, $P < 0.05$, (*D*) n = 7 to 17] (*I* and *J*) n = 50 sets of MTs for all treatments (n = 3 per treatment). (*K*) Fluid secretion rates were measured at 10-min intervals initially over a 30-min interval (unstimulated) and then over a second 30-min interval after the addition (solid arrow) of 10^{-4} M cAMP or 10^{-8} M cGMP. Significant differences between cAMP-treated MTs and the corresponding time point controls (or cGMP-treated MTs) are denoted by an asterisk (mean ± SEM; two-way ANOVA with Bonferroni multiple comparison, $P < 0.05$, n = 5 to 6). (*L*) Significant differences between cAMP-treated MTs and corresponding time point after addition at 30 min (downward arrow) of cGMP are denoted by an asterisk (similar with cGMP alone and cAMP added at 30 min, mean ± SEM; one-way ANOVA with Bonferroni multiple comparison, $P < 0.05$, n = 5 to 9).

changes in either secretion rate (*SI Appendix*, Fig. S1*B*) or pH (*SI Appendix*, Fig. S1*C*).

***Aedae*CAPA-1 Increases cGMP and Decreases cAMP Levels in DH_{31}-Treated MTs.** To further clarify the CAPA signaling pathway involving the second messengers, cGMP and cAMP, we sought to determine changes in levels of these cyclic nucleotides in MTs incubated in DH_{31} alone or combined with *Aedae*CAPA-1. Treatment of MTs with DH_{31} alone had basal levels of cGMP, 10.91 ± 0.109 $pmol^{-1}$/tubule, comparable to saline-treated MTs (Fig. 1*I*). Treatment of MTs with *Aedae*CAPA-1 resulted in a significant increase in cGMP levels compared to DH_{31}– incubated tubules, increasing to 11.39 ± 0.101 $pmol^{-1}$/tubule. Similar results were observed with MTs treated with both DH_{31}+ *Aedae*CAPA-1, with significantly increased cGMP levels of 11.39 ± 0.123 $pmol^{-1}$/tubule (Fig. 1*I*) compared to MTs treated with DH_{31} alone. In contrast, treatment of MTs with DH_{31} alone led to significantly higher levels of cAMP, 9.153 ± 0.039 $pmol^{-1}$/tubule, while baseline levels of this second messenger were observed in saline, DH_{31}+ *Aedae*CAPA-1, and *Aedae*CAPA-1 treated tubules (Fig. 1*J*). To further confirm the stimulatory role of cAMP and inhibitory role of cGMP, tubules were treated with either cyclic nucleotide alone and secretion rates were measured (Fig. 1*K*). Unstimulated fluid secretion rates were measured over the first 30 min, and then at 10-min intervals with either cAMP or cGMP. Treatment of MTs with 10^{-4} M cAMP led to a significant increase over the treatment interval, with fluid secretion rates increasing to 0.615 ± 0.096 nL min^{-1} at 60 min, compared to 10^{-8} M cGMP (0.052 ± 0.091 nL min^{-1}) and unstimulated (0.065 ± 0.091 nL min^{-1}) (Fig. 1*K*). Finally, to establish whether these cyclic nucleotide second messengers elicit antagonistic control of the MTs in adult *A. aegypti*, tubules were treated initially with cAMP over the first 30 min and then cGMP was added in the presence of cAMP for a subsequent 30 min (Fig. 1*L*). Similarly, we also tested the opposite treatment regime where MTs were treated initially with cGMP and subsequently with cAMP added along with cGMP.

Treatment of cAMP-stimulated MTs with 10^{-8} M cGMP led to a significant decrease (~fourfold) over the treatment interval, with secretion rates decreasing to 0.231 ± 0.113 nL min^{-1} at 60 min, compared to 10^{-4} M cAMP alone (0.931 ± 0.134 nL min^{-1}). In contrast, cGMP-incubated tubules treated with 10^{-4} M cAMP led to a significant increase (~10-fold) in secretion rate (0.537 ± 0.072 nL min^{-1}) compared to MTs treated with 10^{-8} M cGMP alone (0.045 ± 0.018 nL min^{-1}) (Fig. 1*L*).

Parallel studies examining cAMP levels were measured in DH_{44}-incubated MTs. Treatment of MTs with DH_{44} alone had high levels of cAMP, 9.115 ± 0.0.061 $pmol^{-1}$/tubule, compared to saline-treated MTs, 8.709 ± 0.081 $pmol^{-1}$/tubule (*SI Appendix*, Fig. S2*A*). Levels of cAMP remained unchanged in tubules treated with both DH_{44}+ *Aedae*CAPA-1, 8.954 ± 0.108 $pmol^{-1}$/tubule. To further resolve the cAMP signaling pathway downstream of DH_{31}- and DH_{44}-stimulated diuresis, a PKA inhibitor (KT5720) was tested against diuretic-stimulated MTs. KT5720 abolished the stimulatory effect of DH_{31}, whereas secretion rates by DH_{44}-treated MTs remained unchanged (*SI Appendix*, Fig. S2*B*).

In *D. melanogaster*, the effects of CAPA peptides are dependent on both intracellular and extracellular sources of Ca^{2+} (9, 37). Thus, we sought to test the involvement of Ca^{2+} in the CAPA intracellular second messenger pathway in the *Aedes* mosquito. The tubules were tested in a modified Ca^{2+}-free saline containing L-glutamine, resulting in secretion rates similar to MTs incubated in Ca^{2+}-free saline with Schneider's medium and *Aedes* saline used previously (*SI Appendix*, Fig. S3*A*). Treatment of MTs in the presence of the Ca^{2+}-chelating agent EGTA had no effect on the inhibition of DH_{31}-stimulated secretion by *Aedae*CAPA-1 (*SI Appendix*, Fig. S3*B*). Similarly, inhibition of intracellular Ca^{2+} levels with TMB-8 or membrane-permeable BAPTA-AM alone or in combination with EGTA had no effect on the antidiuretic activity of *Aedae*CAPA-1 (*SI Appendix*, Fig. S3*B*).

***Aedae*CAPA-1 Decreases VA Activity in DH_{31}-Stimulated MTs through the NOS/cGMP/PKG Pathway.** In *Aedes* MTs, 50 to 60% of the total ATPase activity can be attributed to a bafilomycin- and nitrate-sensitive component that reflects the activity of the VA pump (13). The remaining ATPase activity may be due to nucleotide cyclases, protein kinases, myosin, DNA helicases, and other ATP-consuming processes such as the NKA (13). As such, to determine whether CAPA inhibits VA and/or NKA function in the female mosquito, diuretic-stimulated MTs were challenged with *Aedae*CAPA-1 to measure the resultant NKA and VA activity. As expected, given its established role as the natriuretic diuretic hormone, adult female MTs treated with DH_{31} resulted in a significant (over twofold) increase of VA activity, 0.0329 ± 0.0007 µmoles ADP/µg protein/hour, compared to saline controls, 0.0151 ± 0.0021 µmoles ADP/µg protein/hour (Fig. 2*A*). Importantly, MTs incubated with both DH_{31} and *Aedae*CAPA-1 had significantly lower VA activity, resulting in activity levels indistinguishable from saline controls. In contrast, neither 5HT nor DH_{44} influenced VA activity ($P > 0.05$) when compared with saline controls, while cotreatment with *Aedae*CAPA-1 also resulted in indistinguishable VA activity. Similar VA activity levels were observed between 5HT and DH_{44} (0.0255 ± 0.0078 and 0.0208 ± 0.0042 µmoles ADP/µg protein/hour) and with coapplication of *Aedae*CAPA-1 (0.0150 ± 0.0036 and 0.0154 ± 0.0070 µmoles ADP/µg protein/hour). Unlike changes observed in VA activity following treatment with DH_{31}, diuretic-stimulation or *Aedae*CAPA-1 treatment did not perturb NKA activity, with levels similar to unstimulated MTs (Fig. 2*B*).

To confirm the actions of CAPA are mediated through the NOS/cGMP/PKG pathway, pharmacological blockers, including inhibitors of NOS ($_L$-NAME) and PKG (KT5823), were tested

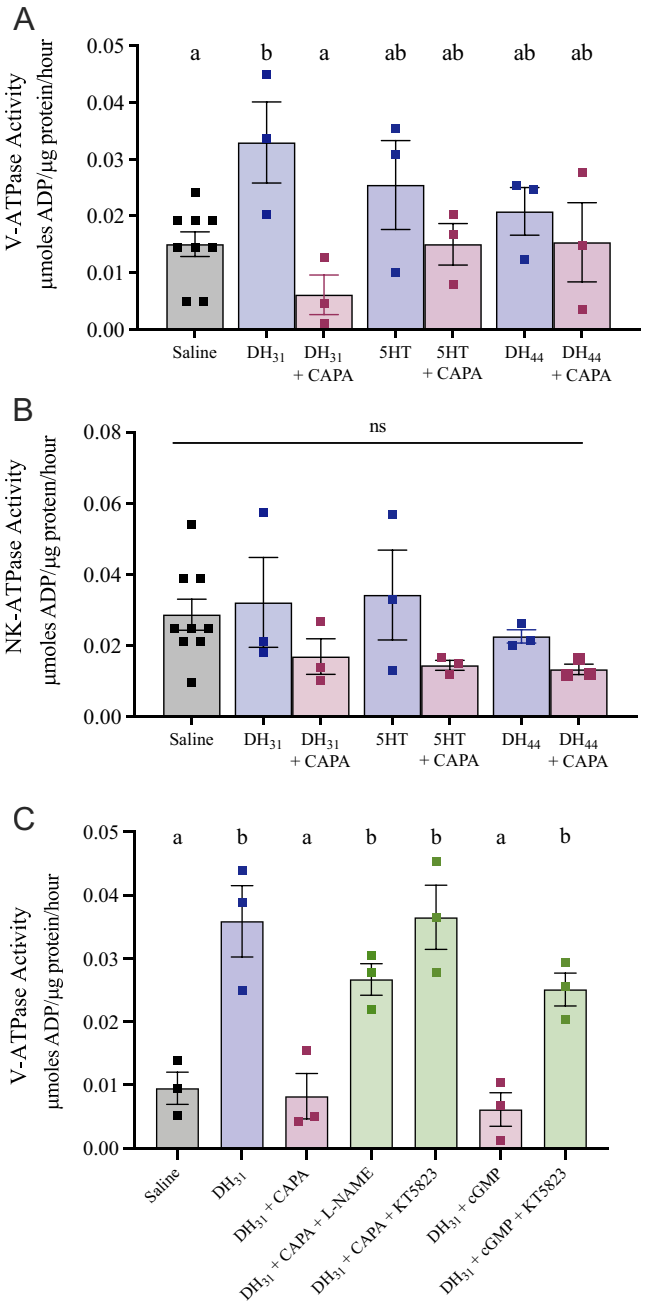

Fig. 2. Effect of *Aedae*CAPA-1 and NOS/PKG inhibitors on VA and NKA activity in diuretic-stimulated *A. aegypti* MTs. MTs were incubated in *Aedes* saline, diuretics (DH_{31}, 5HT, and DH_{44}) alone or in combination with *Aedae*CAPA-1 for 30 min before collection to measure (*A*) VA and (*B*) NKA activity. (*C*) MTs were treated with pharmacological blockers, NOS inhibitor ($_L$-NAME) and PKG inhibitor (KT5823) in combination with either *Aedae*CAPA-1 or cGMP. Bars labeled with different letters are significantly different from each other (mean ± SEM; one-way ANOVA with Bonferroni multiple comparison, $P < 0.05$). N.S. denotes no statistical significance. For each treatment, 50 sets of MTs were collected with n = 3 biological replicates per treatment.

against DH_{31}-stimulated MTs treated with either *Aedae*CAPA-1 or cGMP (Fig. 2*C*). Application of $_L$-NAME or KT5823 abolished the inhibitory effect of *Aedae*CAPA-1, resulting in high levels of VA activity, 0.02671 ± 0.0025 and 0.03653 ± 0.0051 µmoles ADP/µg protein/hour respectively, compared to MTs treated with DH_{31}+ *Aedae*CAPA-1. As expected, treatment of DH_{31}-stimulated MTs with cGMP resulted in a significant decrease in VA activity, 0.006 ± 0.0026 µmoles ADP/µg protein/hour, similar to *Aedae*CAPA-1-treated MTs, while cotreatment with KT5823,

abolished the inhibitory effect of cGMP, resulting in an increase in VA activity (Fig. 2*C*).

***Aedae*CAPA-1 Leads to VA Holoenzyme Dissociation in DH_{31}-Treated MTs.** The reversible dissociation of the V_1 complex from the V_o membrane-integrated complex is a well-known mechanism for regulating VA transport activity (22, 31, 34, 35, 38). To determine whether *Aedae*CAPA-1 influences VA complex dissociation, membrane and cytosolic protein fractions were isolated from DH_{31} and DH_{31}+ *Aedae*CAPA-1 incubated MTs, and a polyclonal V_1 antibody (13) was used to measure protein abundance. First, membrane and cytosolic protein isolation was verified with specific membrane (AQP1, *SI Appendix*, Fig. S4*A*) and cytosolic (beta-tubulin, *SI Appendix*, Fig. S4*B*) markers. Western blot analysis revealed three protein bands, with calculated molecular masses of 74 kDa, 56 kDa, and 32 kDa (13, 39) (*SI Appendix*, Fig. S4*C*). The V_1 complex is composed of eight subunits (A to H), which includes the A (~74 kDa) and B subunit (~56 Da) that are arranged in a ring forming the globular headpiece for ATP binding and hydrolysis (31). Additionally, studies have suggested that subunit D (~32 kDa) alongside subunit F constitute the central rotational stalk of the V_1 complex (17). There was no difference in abundance observed for the A subunit (74-kDa band) in either membrane or cytosolic fractions between saline and DH_{31} treatments whereas DH_{31}+ *Aedae*CAPA-1 incubated MTs had increased A subunit (74-kDa band) protein abundance in cytosolic fractions compared to saline treatment (Fig. 3*A*) and decreased abundance in the membrane fraction compared to MTs treated with DH_{31} alone (Fig. 3*B*). Similarly, the V_1 complex B subunit abundance (56-kDa band) was similar in all treatments within the cytosolic protein fraction (Fig. 3*C*) whereas DH_{31}+ *Aedae*CAPA-1 incubated MTs had significantly lower abundance in membrane fractions

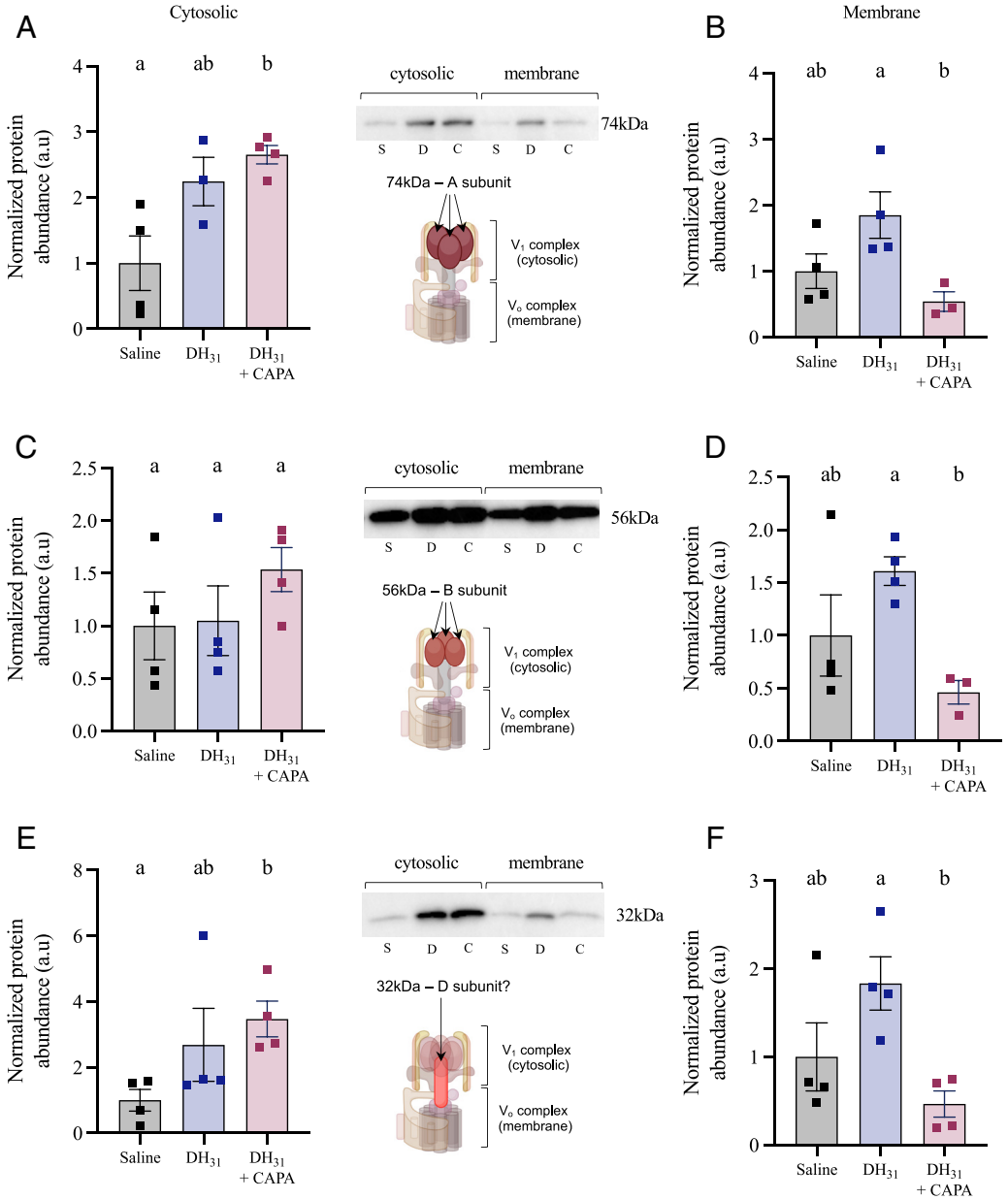

Fig. 3. Membrane and cytosolic protein abundance of the V_1 complex in MTs of *A. aegypti*. The MTs (n = 40 to 50) were incubated in *Aedes* saline, DH_{31}, or DH_{31}+ *Aedae*CAPA-1 for 1 h before collection. Cytosolic and membrane protein abundance was measured in the (*A* and *B*) 74-kDa band, A subunit, (*C* and *D*) 56-kDa band, B subunit, and (*E* and *F*) 32-kDa band, D subunit of the V_1 complex. Individual band densities were normalized to total protein using Coomassie staining and graphed relative to saline-treated controls. Bars labeled with different letters are significantly different from each other (mean ± SEM; one-way ANOVA with Bonferroni multiple comparison, $P < 0.05$, n = 3 to 4 replicates).

compared to MTs treated with DH_{31} alone (Fig. 3*D*). Finally, there was no difference in abundance of the V_1 complex subunit D (32-kDa band) between saline and DH_{31}-treated MTs in neither cytosolic nor membrane fractions. However, as observed for the A and B subunit bands (74- and 56-kDa bands, respectively) DH_{31}+ *Aedae*CAPA-1 incubated MTs showed a significant increase in subunit D abundance in cytosolic fractions compared to saline-treated MTs (Fig. 3*E*) and a decrease in its abundance in membrane fractions compared to MTs treated with DH_{31} alone (Fig. 3*F*). In summary, all three of the V1 complex immunoreactive bands corresponding to subunits A, B, and D (74, 56, and 32 kDa, respectively) showed significantly lower abundance in membrane fractions in DH_{31}+ *Aedae*CAPA-1 incubated MTs.

To visualize this potential endocrine-mediated reorganization of the VA holoenzyme in this simple epithelium, we immunolocalized the membrane-integrated V_o and cytosolic V_1 complex in the female *A. aegypti* MTs. Transverse sections of saline-incubated (control) MTs demonstrated moderate enrichment of V_o (Fig. 4*A* and *SI Appendix*, Fig. S5*A*), and V_1 (Fig. 4*B* and *SI Appendix*, Fig. S5*B*) complexes in the apical membrane of principal cells (Fig. 4*C* and *SI Appendix*, Fig. S5 *C* and *D*). Comparatively, DH_{31}-incubated MTs revealed intense localization of the V_o (Fig. 4*D* and *SI Appendix*, Fig. S5*E*), and V_1 (Fig. 4*E* and *SI Appendix*, Fig. S5*F*) complexes within principal cells, where V_1 staining was strictly colocalized with V_o staining on the apical membrane (Fig. 4*F* and *SI Appendix*, Fig. S5 *G* and *H*). Interestingly, although V_o immunolocalization was restricted to the apical membrane (Fig. 4*G* and *SI Appendix*, Fig. S5 *I–K*), V_1 immunoreactivity was dispersed in both the apical membrane and cytosolic region (Fig. 4*H* and *SI Appendix*, Fig. S5 *L–N*) in DH_{31}+ *Aedae*CAPA-1 treated MTs with little evidence of apical colocalization (Fig. 4*I* and *SI Appendix*, Fig. S5 *O–T*) as observed in MTs treated with DH31 alone. Immunostaining was absent in control preparations probed with only secondary antibodies (*SI Appendix*, Fig. S6 *A* and *B*) confirming the specific detection of the VA complexes with each primary antibody. Additionally, to further resolve the involvement of the cGMP/PKG pathway in VA holoenzyme organization, DH_{31}- and cAMP-stimulated tubules were incubated with cGMP alone or with PKG blocker, KT5823 (*SI Appendix*, Fig. S7). As expected, transverse sections of both DH_{31}- and cAMP-incubated MTs demonstrated strict colocalization of V_o (*SI Appendix*, Fig. S7 *A* and *J*) and V_1 (*SI Appendix*, Fig. S7 *B* and *K*) in the apical membrane of principal cells (*SI Appendix*, Fig. S7 *C* and *L*), while V_1 and V_o immunoreactivity was found in both the apical membrane and cytosol regions in cAMP + cGMP and DH_{31}+ cGMP cotreated MTs (*SI Appendix*, Fig. S7 *D–F* and *M–O*). However, immunoreactivity of the V_1 complex was found in the apical membrane alongside the V_o complex in preparations treated with the PKG blocker, KT5823 (*SI Appendix*, Fig. S7 *G–I* and *P–R*).

To investigate this endocrine-mediated phenomenon in vivo, we immunolocalized the membrane-integrated V_o and cytosolic V_1 complex in blood-fed females at different time points. Whole body sections of non-blood-fed similarly aged females (control) demonstrated moderate enrichment of both V_o (Fig. 5*A*), and V_1 (Fig. 5*B*) in the MTs, with minimal colocalization (Fig. 5*C*), resembling saline-incubated MTs. Interestingly, blood-fed female MTs revealed strong colocalization of the V_o and V_1 complexes at 10 min (Fig. 5 *D–F*) and 30 min (Fig. 5 *G–I*) post blood meal, whereas V_1 immunoreactivity was more dispersed in both the apical membrane and cytosolic area in MTs 3 h post blood meal (Fig. 5 *J–L*), comparable to non-blood-fed females.

Discussion

The MTs of the *Aedes* mosquito are the main organs responsible for the secretion of water and solutes, thereby contributing toward hydromineral homeostasis of the animal (40). Active ion transport in *A. aegypti* MTs is accomplished mainly by the V-ATPases (VA) densely localized in the apical brush-border membrane of principal cells, that energize the apical and basolateral membrane as well as the paracellular pathway, allowing for transepithelial secretion of NaCl, KCl, and other solutes (41). In animal cells, VA localized to the plasma membrane, especially on the apical membrane of epithelial cells, contribute to extracellular acidification or alkalization,

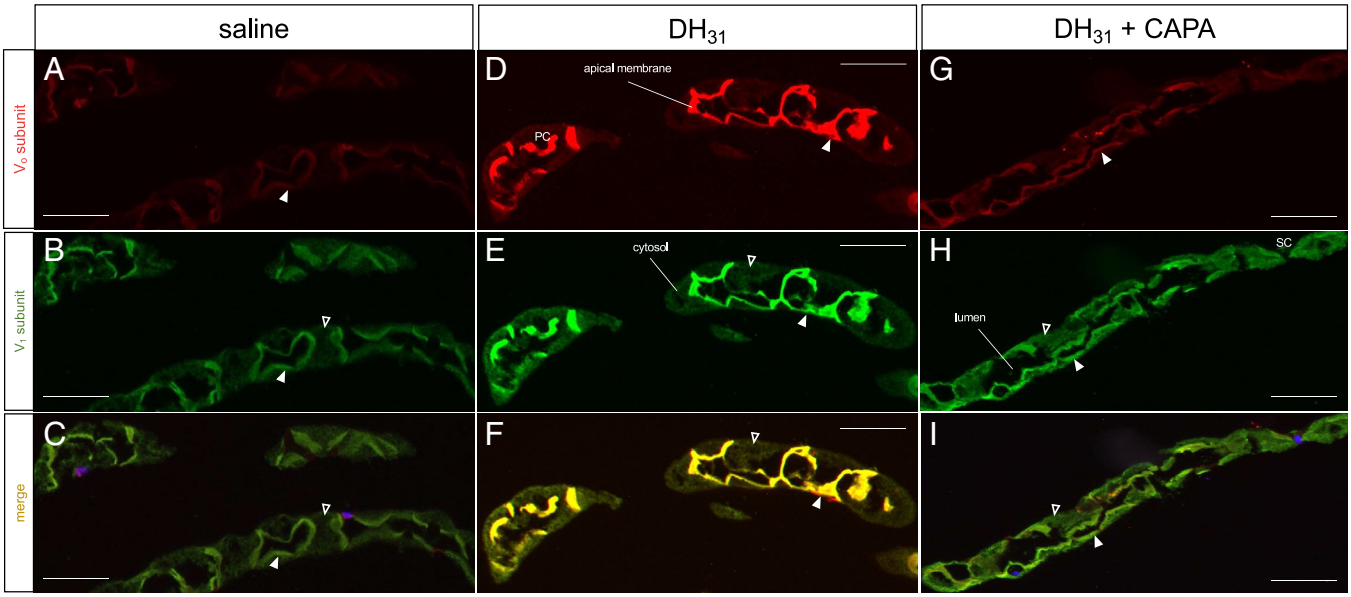

Fig. 4. Immunolocalization of the V_o and V_1 complexes in transverse sections of stimulated *A. aegypti* MTs. Representative paraffin-embedded sections of *A. aegypti* MTs incubated in either (*A–C*) *Aedes* saline alone, (*D–F*) DH_{31} and (*G–I*) DH_{31}+ *Aedae*CAPA-1 for 30 min. Panels (*A*, *D*, and *G*) show V_o staining (red), (*B*, *E*, and *H*) show V_1 staining (green), and panels (*C*, *F*, and *I*) show merged images with staining highly colocalized in DH_{31} treatment but less evident in saline and *Aedae*CAPA-1 added treatments. Solid white arrows denote apical VA staining, and empty arrows indicate cytosolic VA staining. Where visible in sections, DAPI nuclear staining is shown in blue. Scale bar 100 μm, n = 4 biological replicates (SC = stellate cell).

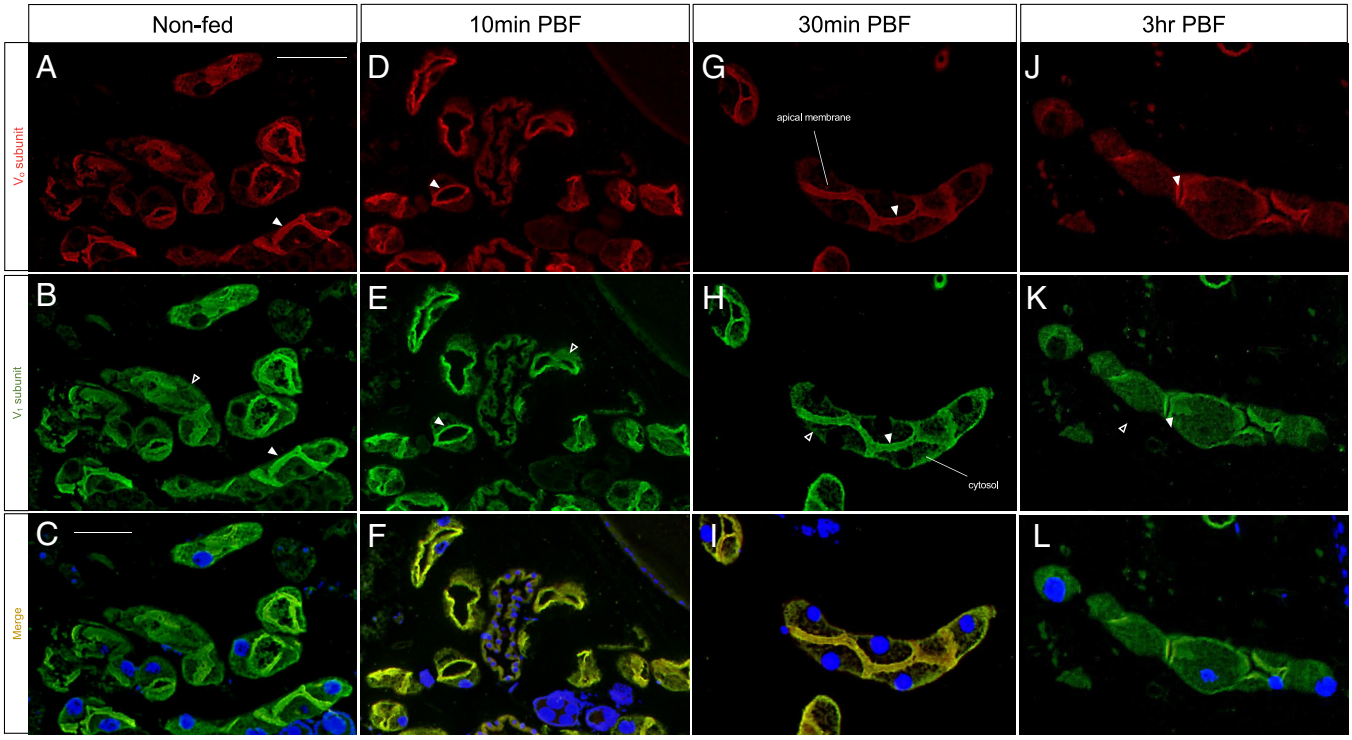

Fig. 5. Immunolocalization of the V_o and V_1 complexes in blood-fed *A. aegypti* females. Representative paraffin-embedded sections of whole-body non-blood-fed females (*A*–*C*), blood-fed females isolated (*D*–*F*) 10 min (*G*–*I*) 30 min and (*J*–*L*) 3 h post blood meal. Panels (*A*, *D*, *G*, and *J*) show V_o staining (red), (*B*, *E*, *H*, and *K*) show V_1 staining (green), and panels (*C*, *F*, *I*, and *L*) show merged immunoreactive staining. DAPI nuclear staining is shown in blue. Scale bar 100 μm, n = 4 biological replicates.

intracellular pH homeostasis, or energize the plasma membrane for secondary active transport (42, 43). In insect MTs, the VA plays a major role in fluid secretion, thus serving as a primary target for both diuretic and, as this study demonstrates, antidiuretic hormonal regulation of the mosquito renal tubules. Although the structure and function of the VA has been elucidated in some detail (13, 20, 22, 31, 44–46), the regulation of the proton pump remains unclear. Of the various regulatory mechanisms for VA activity, the most studied is the reversible dissociation of the cytosolic V_1 complex from the membrane-integrated V_o complex, first established in the midgut of the tobacco hornworm, *Manduca sexta,* and yeast, *Saccharomyces cerevisiae* (45, 47). In this study, the activity and regulation of the VA was investigated under both diuretic and antidiuretic hormone control of the adult female *A. aegypti* MTs. Notably, the current results advance our knowledge of the antidiuretic control of the *A. aegypti* MTs, revealing a cellular mechanism for CAPA inhibition of the MTs by targeting the VA to block fluid secretion stimulated by select diuretic factors. This includes inhibition of the DH_{31}-related mosquito natriuretic peptide, which is critical for the post-hematophagy diuresis that eliminates excess water and sodium originating from the blood meal–derived plasma.

In insects, water excretion is tightly regulated to maintain homeostasis of ions and water (1, 48, 49). Female *A. aegypti* engorge a salt- and water-rich blood meal to obtain the necessary nutrients and proteins for their eggs (1), with about 40% of the ingested water eliminated in the first hour postfeeding (50). The high rates of water excretion along with the high rates of primary urine production post blood meal suggest a highly coordinated and defined hormonal regulation of the signaling processes and downstream cellular targets for ion and water transport (51). In *Aedes* MTs, fluid secretion increases at least threefold after stimulation with mosquito natriuretic peptide (identified as DH_{31}), using cAMP as a second messenger (1), activating PKA, which subsequently activates V-ATPase-driven cation transport processes (22, 35, 39). Herein we show that DH_{31}-stimulated secretion is inhibited by bafilomycin, which blocks the proton channel of the VA (32). Moreover, the addition of either bafilomycin or *Aedae*CAPA-1 caused alkalization of the secreted fluid, indicating inhibition of the VA, which may lead to constrained entry of cations across the apical membrane through a proposed alkali cation/proton antiporter (15, 16). Thus, since bafilomycin inhibits DH_{31}-stimulated secretion, this supports the VA as a target in the inhibition of fluid secretion. Consequently, the driving force for ion movement and osmotically obliged water is reduced, but select Na^+ channels and cotransporters remain unaffected in the presence of *Aedae*CAPA-1, as observed by the unchanged natriuretic effect of DH_{31} despite reduced secretion rates in response to *Aedae*CAPA-1 (4). Similar results were seen in 5HT-stimulated secretion, albeit a partial inhibition. An earlier study demonstrated that Ca^{2+}-mediated diuresis does not require the assembly and activation of the VA (38, 39). The cAMP effect on the VA is implemented by protein kinase A (PKA), with inhibitors of PKA abolishing hormone-induced assembly and activation of the VA (34). Although the endogenous 5HT receptor expressed within the *A. aegypti* MTs necessary for diuretic activity remains elusive, in the kissing bug, *Rhodnius prolixus*, both cAMP and Ca^{2+} have been shown to initiate diuresis in response to 5HT (52), which might explain the partial inhibitory response of *Aedae*CAPA-1 inhibition on 5HT-stimulated tubules as Ca^{2+}-mediated diuresis is independent of the VA (39). Notably, the anticipated 5HT type 2 receptor subtype expressed in the principal cells of the MTs is predicted to couple through a Gq/11 signaling mechanism (53) and likely excludes the type 7 Gs-coupled receptor localized to tracheolar cells associated with the MTs (54, 55) as well as the type 1 Gi-coupled receptor localized to principal cells in larval stage mosquitoes (56).

Interestingly, DH_{44}-mediated stimulation was observed to be independent of the VA, as bafilomycin had no effect on the secretion rate or pH of the secreted fluid following application of this CRF-related diuretic peptide. Previous studies have noted that low nanomolar concentrations of a DH_{44}-related peptide were linked to the stimulation of the paracellular pathway only (27), mediating this action through intracellular Ca^{2+} as a second messenger (57). In contrast, high nanomolar concentrations of a DH_{44}-related peptide were shown to influence both paracellular and transcellular transport, increasing intracellular Ca^{2+} and cAMP (57). Although haemolymph concentrations of diuretic peptides have yet to be determined in mosquitoes, DH_{31} is immediately released into circulation post blood meal, stimulating rapid secretion of Na^+ and excess water (23, 50). In contrast, DH_{44}-stimulated diuresis in *A. aegypti* involves nonselective transport of Na^+ and K^+ cations (4); this supports a delayed release of this diuretic hormone post-feeding to maintain production (albeit reduced) of primary urine while conserving Na^+ ions.

In unstimulated adult female *Aedes* MTs isolated in vitro, the VA exhibits variable rates of enzyme activity, consistent with highly variable rates of secretion, as found also in various other insect species (26, 58, 59). The VA is the main energizer in MTs as 60% of total ATPase activity can be linked to the VA (13), whereas the NKA, with around 28% of ATPase activity, also plays a role in membrane energization, denoting a more important role in the function of MTs than was previously assumed (19, 39–41). Here, we show a significant twofold increase in VA activity in MTs treated with DH_{31} compared to the unstimulated MTs, with no change in VA activity in 5HT and DH_{44}-treated MTs. Notably, *Aedae*CAPA-1 treatment blocked the DH_{31}-driven increase in VA activity, which corroborates the reduced fluid secretion rate and alkalization of the secreted fluid. Additionally, we sought to establish the importance of the NOS/cGMP/PKG pathway in the inhibitory actions of *Aedae*CAPA-1 on VA association. In stimulated MTs treated with *Aedae*CAPA-1 along with NOS inhibitor, $_L$-NAME, or PKG inhibitor, KT5823, the inhibitory activity of *Aedae*CAPA-1 and its second messenger cGMP was abolished, resulting in elevated VA activity as a result of DH_{31} treatment. The present study examined the effects of *Aedae*CAPA-1 on DH_{31}-stimulated VA activation in insects. Stimulation of DH_{31} causes an increase in cAMP production, which activates Na^+ channels and the $Na^+/K^+/2Cl^-$ cotransporter in the basolateral membrane (60) and up-regulates VA activity (as shown herein and previously) critical for increased fluid secretion (24). The DH_{31} receptor (*Aaeg*GPRCAL1) is expressed in a distal-proximal gradient in the MTs, with greater expression in principal cells where the VA in the apical membrane is highly expressed (19, 61). The colocalization of the DH_{31} receptor, VA, and cation exchangers (62–64) in the distal segment of the MTs, along with the CAPA receptor (6), collectively supports the major roles DH_{31} and CAPA play in postprandial diuresis and antidiuresis, respectively. In contrast to the marked changes in VA activity in response to diuretic and antidiuretic hormones, NKA activity remained unchanged in response to treatments conducted herein. Further studies should examine the potential role of the NKA in diuretic and antidiuretic processes.

The reversible dissociation of the V_1 and V_o complexes is currently thought of as a universal regulatory mechanism of V-ATPases, appearing to be widely conserved from yeast to animal cells (13, 22, 35, 65). Although previously shown with cAMP (24), it remained unclear whether other second messengers (e.g., Ca^{2+}, cGMP, and nitric oxide) affect the assembly/disassembly of the V_1V_o complexes in insect MTs. In this study, VA protein abundance in membrane and cytosolic fractions of MTs was confirmed by immunoblot analyses. The 56-kDa band represents the B subunit (29), while the 74-kDa and 32-kDa bands are suggested to be the A and D subunits, respectively, of the V_1 complex (36). The higher abundance of these V_1 complex protein subunits in the cytosolic fraction and lower abundance in membrane fraction in *Aedae*CAPA-1-treated MTs provide evidence of hormonally regulated V_1 dissociation from the holoenzyme in *A. aegypti* MTs. This was further confirmed with V_1 staining found both in the apical membrane and cytosol of the MTs treated with DH_{31} and *Aedae*CAPA-1 in contrast to the strict colocalization of the V_1 and V_o complex in the apical membrane of MTs treated with DH_{31} alone. This strict colocalization of the VA complex in both DH_{31}- and cAMP-treated MTs was further abolished in the presence of cGMP, however, rescued with the addition of the PKG inhibitor, KT5823. In unstimulated *A. aegypti* MTs, 40 to 73% of the V_1 subunits were found to be membrane associated, with reassembly of the V_1V_o complex observed upon stimulation with cAMP analogs (39). Although studies have revealed that hormonal regulation can activate the assembly of the holoenzyme, the signaling mechanisms achieving this control are unclear. In this study, the data provide strong evidence of VA assembly in DH_{31}-treated MTs, with V_1 complex protein subunit enrichment found in the membrane fractions, confirming the crucial role of the VA in DH_{31}-stimulated secretion. Studies in *A. aegypti* have demonstrated the involvement of PKA in the activation and assembly of the VA upon natriuretic hormone (i.e., DH_{31}) stimulation and indicate the phosphorylation of the VA subunits by PKA in the MTs (39). These studies indicate a regulatory role of PKA in VA assembly and its activation that may be independent or in addition to phosphorylation (39). In line with these earlier observations, the current results indicate PKA is critical for DH_{31}-stimulated fluid secretion by MTs.

Together, these results indicate that *Aedae*CAPA-1 binds to its cognate receptor in principal cells of the adult *A. aegypti* mosquito MTs (6), targets the NOS/cGMP/PKG pathway (4, 6) to inhibit DH_{31}-mediated elevation of cAMP (23, 60), which blocks PKA-activated VA association and prevents protons from being pumped across the apical membrane, resulting in a more alkaline lumen. Additionally, in female *Aedes* MTs, the effect of CAPA peptides is independent of Ca^{2+}, which is in contrast to *Drosophila* MTs, where CAPA peptide diuretic activity involves modulation of intracellular concentrations of Ca^{2+}, which can derive from both extracellular and intracellular sources of this important signaling molecule (see ref. 9). Our study provides evidence that the antidiuretic activity of CAPA is mediated through the dissociation of the VA holoenzyme involving the removal of the V_1 complex from the apical membrane, hindering luminal flux of protons that in turn starves cation/H^+ exchange, which ultimately reduces fluid secretion (Fig. 6). CAPA peptides are known to elicit both diuretic and antidiuretic actions in different insects, whereby a stimulatory role has been established in *D. melanogaster* (9, 10) and inhibitory in the *R. prolixus* (65) and *D. melanogaster* (11, 12) indicating a species-specific role of this neuropeptide family, which may be due to their different diets and lifestyles. Given the unique blood-feeding stress the female mosquito is subjected to, a carefully controlled mechanism of both diuretic and antidiuretic hormones is warranted to rid the haemolymph of excess salts and water while also preventing the female from excessive secretion.

In *R. prolixus* MTs, the physiological roles of cGMP and cAMP were examined (66) suggesting cGMP inhibits fluid secretion by activating a phosphodiesterase (PDE) that degrades cAMP elevated following 5HT and diuretic hormone stimulation of MTs. Indeed, the current results demonstrated the addition of cAMP reversed the inhibitory effects of cGMP, while the addition of cGMP reduced the stimulatory response of cAMP, supporting that these two cyclic nucleotides

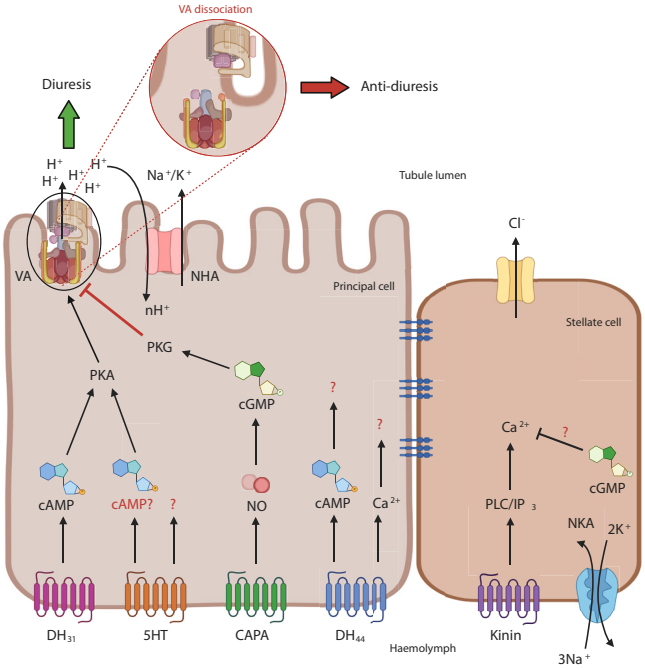

Fig. 6. Schematic diagram summarizing the signaling pathway of diuretic and antidiuretic control of adult *A. aegypti* MTs. The principal cells in *A. aegypti* MTs are responsible for the transport of Na^+ and K^+ cations via secondary active transport, energized by the V-type H^+-ATPase (VA), localized in the brush border of the apical membrane. The movement of protons creates a gradient, driving the exchange of Na^+ and K^+ through cation/H^+ antiporters (NHA). Neurohormone receptors for DH_{31}, 5HT, DH_{44}, and CAPA are localized to the basolateral membrane of the principal cells, while the kinin receptor is localized exclusively in the stellate cells. The current results together with previous data indicate that DH_{31} stimulates diuresis through activation and assembly of the VA in the apical membrane, with no effect on the Na^+/K^+-ATPase (NKA). The antidiuretic effect of *Aedae*CAPA-1, facilitated by the NOS/cGMP/PKG pathway, causes V_1 dissociation from the membrane, hindering activity, and thus reducing fluid secretion. The biogenic amine, 5HT, has also been shown to stimulate activation of the VA, however, to a lesser extent. DH_{44}-related peptide receptor activation increases Ca^{2+} (as well as cAMP at higher doses), but its action was found to be independent of PKA and VA. Lastly, it was shown earlier that cGMP inhibits kinin-stimulated diuresis, suggesting that an additional antidiuretic factor may exist that acts specifically on stellate cells.

facilitate two opposing regulatory roles in the MTs of adult *A. aegypti*. The data herein reveals cGMP levels increase in MTs treated with CAPA alone or in combination with DH_{31} while cAMP levels decrease in MTs treated with CAPA in combination with DH_{31} compared to tubules stimulated with DH_{31} alone, which upholds the roles of cAMP and cGMP in diuretic and antidiuretic signaling pathways, respectively. Interestingly, mid-nanomolar concentrations of DH_{44} also led to increased levels of cAMP, with levels unchanging in response to *Aedae*CAPA-1, raising doubt regarding the involvement of a PDE. While treatment of a PKA inhibitor, KT5720, abolished DH_{31}-stimulated secretion, no effect was observed in DH_{44}-mediated stimulation. Thus, despite DH_{44}-stimulated diuresis was found to involve increased cAMP, it appears to be PKA-independent. It is well established that the effects of cAMP are mediated by activation of cAMP-dependent protein kinase (PKA), a major cAMP target, followed by phosphorylation of target proteins (67). More recently, in *D. melanogaster* MTs, two distinct cAMP pathways have been elucidated to sustain fluid secretion; a PKA-dependent pathway, shown to regulate basal fluid secretion in principal cells; and a PKA-independent pathway, specifically a stimulatory principal EPAC (exchange proteins directly activated by cAMP) pathway, stimulating fluid secretion above basal levels (68). Future studies should examine the DH_{44} diuretic pathway leading to secretion in *A. aegypti* MTs that appears to be PKA-independent and functions in the absence of VA activation.

In summary, our study highlights a target in the antidiuretic signaling pathway of adult female *A. aegypti* MTs, emphasizing the intricate and precise regulatory mechanism of antidiuresis. Although a plethora studies have investigated the process of hydromineral balance in terrestrial insects from a diuretic perspective (1, 10, 23, 65, 69–71), these current findings advance our understanding of antidiuretic hormone control while providing further evidence of a previously elusive endocrine regulatory mechanism of the VA in mosquitoes (Fig. 6). Given that many insects are recognized as agricultural pests or disease vectors, further investigating the complex regulation of their ionic and osmotic balance may aid in lessening their burden on human health and prosperity through development of improved management strategies that, at least in part, impede their neuroendocrine control of hydromineral homeostasis.

Materials and Methods

Animal Rearing. Eggs of *A. aegypti* (Liverpool strain) were collected from an established laboratory colony described previously (4, 72). All mosquitoes were raised under a 12:12 light:dark cycle. Non-blood-fed female insects (3 to 6 d posteclosion) were used for bioassays, dissected under physiological saline (*Aedes* saline) adapted from ref. 60 that contained (in $mmol^{-1}$): 150 NaCl, 25 HEPES, 3.4 KCl, 7.5 NaOH, 1.8 $NaHCO_3$, 1 $MgSO_4$, 1.7 $CaCl_2$, and 5 glucose, and titrated to pH 7.1.

MT Fluid Secretion Assay. In order to determine fluid secretion rates, modified Ramsay assays were performed as described previously (4, 73). Female adults (3 to 6 d old) were dissected under physiological *Aedes* saline prepared as described above, and MTs were removed and placed in a Sylgard-lined Petri dish containing 20 µL bathing droplets (1:1 mixture of Schneider's Insect Medium (Sigma-Aldrich): *Aedes* saline, immersed in hydrated mineral oil to prevent evaporation. The proximal end of each tubule was wrapped around a Minutien pin to allow for fluid secretion measurements. To investigate the effects of second messengers, cAMP and cGMP, on fluid secretion rate, 10^{-4} M 8 bromo-cAMP (cAMP) (23, 66) and 10^{-8} M 8 bromo-cGMP (cGMP) (4) (Sigma-Aldrich) were used against unstimulated MTs. To test the effects of the pharmacological blocker KT5720 (7) (protein kinase A (PKA) inhibitor), a dosage of 5 µmol L^{-1} (manufacturer's recommended dose) was used against 25 nmol L^{-1} DH_{31}- and 10 nmol L^{-1} DH_{44}-stimulated MTs. To determine the role of second messenger, Ca^{2+}, in the CAPA signaling pathway, MTs were treated in a modified Ca^{2+}-free saline (with and without 9.1 $mmol^{-1}$ L-glutamine) containing (in $mmol^{-1}$): 150 NaCl, 25 HEPES, 3.4 KCl, 7.5 NaOH, 1.8 $NaHCO_3$, 1 $MgSO_4$, and 5 glucose, and titrated to pH 7.1. The role of Ca^{2+} was tested using 1 mmol L^{-1} Ca^{2+} chelator EGTA, 50 µmol L^{-1} (in DMSO) membrane-permeable chelator BAPTA-AM, and 1 nmol L^{-1} intracellular Ca^{2+} chelator 8-(*N*,*N*-diethylamino)octyl 3,4,5-trimethoxybenzoate hydrochloride (TMB-8-HCl) (74).

Time Course Inhibition of Bafilomycin. Dosage of bafilomycin A_1 was based on a dose–response analysis of bafilomycin against DH_{31}-stimulated tubules (*SI Appendix*, Fig. S1). In the interest of determining whether bafilomycin inhibits the effects of the diuretic factors, dosages of 25 nmol L^{-1} *Drome*DH_{31} (~84% identical to *Aedae*DH_{31}) (4, 23, 75), 100 nmol L^{-1} 5HT (4, 70, 76), and 10 nmol L^{-1} *Rhopr*DH (CRF-related diuretic peptide, DH_{44}) (~48% overall identity; ~65% identity and ~92% similarity within the highly conserved N-terminal region to *Aedae*DH_{44}) (4, 57, 77, 78) were applied to the isolated MTs. Neurohormone receptors, including those for 5HT, and the peptides DH_{31}, DH_{44}, and CAPA, are localized to the basolateral membrane of principal cells (6, 55, 60, 79), while the LK receptor is localized exclusively to stellate cells (5). As a result, the effects of bafilomycin were tested on diuretics known to act on the principal cells of the MTs. After incubating with the individual diuretics for 30 min (using the modified Ramsay assay), diuretic peptide was added alone (controls) or in combination with bafilomycin (final concentration 10^{-5} M). The fluid secretion rate was recorded every 10 min for a total of 80 min. In order to determine whether inhibition of the VA was involved in the antidiuretic activity of CAPA peptides on adult MTs, the effects of 1 fmol L^{-1} *Aedae*CAPA-1 (4, 6) were investigated in combination with DH_{31} and bafilomycin.

NKA and VA Activities. The Na^+/K^+-ATPase (NKA) and VA activity in the MTs was determined using a modified 96-well microplate method (80, 81), which relies on the enzymatic coupling of ouabain- or bafilomycin-sensitive hydrolysis of ATP to the oxidation of reduced nicotinamide adenine dinucleotide (NADH). The microplate spectrophotometer is therefore able to directly measure the disappearance of NADH. Adult female MTs (3 to 6 d old) were dissected and incubated for 30 min in *Aedes* saline, diuretic (DH_{31}, 5HT, or DH_{44}) alone or combined with *Aedae*CAPA-1. Following 30-min incubation, MTs were collected into 1.5-mL microcentrifuge tubes (40 to 50 sets of MTs per tube = 200 to 250 MTs per treatment), flash frozen in liquid nitrogen, and stored at −80 °C. To investigate the effects of the pharmacological blockers, a nitric oxide synthase (NOS) inhibitor, N_ω-Nitro-L-arginine methyl ester hydrochloride ($_L$-NAME), and protein kinase G (PKG) inhibitor, KT5823, were used against DH_{31}-stimulated MTs treated with *Aedae*CAPA-1 or 10^{-8} M cGMP. Dosages of 2 μmol L^{-1} $_L$-NAME (manufacturer's recommended dose) and 5 μmol L^{-1} KT5823 were applied to the MTs (4, 6, 7) (see *SI Appendix, Materials and Methods* for assay preparation).

Protein Processing and Western Blot Analyses. MTs were isolated under physiological saline from 40–50 female *A. aegypti* for each biological replicate (defined as n = 1) and incubated for 60 min in the following three treatments: *Aedes* saline, 25 nmol L^{-1} DH_{31}, or 25 nmol L^{-1} DH_{31} + 1 fmol L^{-1} *Aedae*CAPA-1. Following the incubation, tissues were stored at −80 °C until processing. To separate the membrane and cytosolic proteins, a membrane protein extraction kit was used (ThermoFisher Scientific) following recommended guidelines for soft tissue with minor modifications including 200 μL of permeabilization and solubilization buffer and a 1:200 protease inhibitor cocktail (Sigma Aldrich) in both buffers. Final protein concentrations were calculated by Bradford assay (Sigma-Aldrich Canada, Ltd.) according to the manufacturer's guidelines with bovine serum albumin (BioRad Laboratories) as a standard and quantified using an A_o Absorbance Microplate Reader (Azure Biosystems) at 595 nm (see *SI Appendix, Materials and Methods* for western blot analyses).

Immunolocalization of VA Complexes in MTs. Immunohistochemistry of the MTs localizing the VA complexes was conducted following a previously published protocol (82). Adult female MTs (3 to 6 d old) were dissected out in *Aedes* saline and incubated following similar conditions described in the western blot section above. After the incubation, the MTs were immersed in Bouin's solution and fixed for 2 h in small glass vials. To test in vivo changes of the VA complexes, 5- to 6-d-old females were allowed to blood-feed for 20 min (72), after which female mosquitoes were isolated at 10 min, 30 min, and 3 h post blood meal. Similarly aged, non-blood-fed (sucrose-fed) females were isolated as controls. Following the blood meal, whole body females were immersed in Bouin's solution and fixed for 3 h in small glass vials. To test the role of second messengers in VA localization, similarly aged female MTs were incubated in solutions containing 10^{-4} M cAMP, 10^{-8} M cGMP, and 5 μmol L^{-1} KT5823 before being immersed in Bouin's solution and fixed for 2 h. Tissues/whole body females were then rinsed three times and stored in 70% ethanol at 4 °C until further processing. Fixed samples were dehydrated through a series of ethanol washes: 70% ethanol for 30 min, 95% ethanol for 30 min, and 100% ethanol three times for 30 min. The samples were cleared with xylene (ethanol:xylene for 30 min then 100% xylene three times for 30 min), and infiltrated in Paraplast Plus Tissue Embedding Medium (Oxford Worldwide, LLC) at xylene:paraffin wax for 60 min at 60 °C, then rinsed in pure paraffin wax twice for 1 h for 60 °C. Following the last rinse, the samples were embedded in the paraffin wax and left to solidify at 4 °C until further processing. Sections (5 μm) were cut using a Leica RM 2125RT manual rotary microtome (Leica Microsystems Inc.), and slides were incubated overnight on a slide warmer at 45 °C for preparation of immunohistochemistry (*SI Appendix, Materials and Methods*).

cGMP and cAMP Measurements. A competitive cGMP ELISA kit (Cell Signaling Technology, #4360) and cAMP ELISA kit (Cell Signaling Technology, #4339) were used to measure these cyclic nucleotide second messengers from adult *A. aegypti* MTs following different treatments (see *SI Appendix, Materials and Methods* for further details).

Statistical Analyses. Data were compiled using Microsoft Excel and transferred to Graphpad Prism software v.7 to create figures and conduct all statistical analyses. Data were analyzed accordingly using a one-way or two-way ANOVA and a Bonferroni posttest, or Student's *t* test, with differences between treatments considered significant if $P < 0.05$.

Data, Materials, and Software Availability. All study data are openly available at https://doi.org/10.5683/SP3/PADHU5 (83). All other data is included in the article and/or *SI Appendix*.

ACKNOWLEDGMENTS. We sincerely thank Prof. Helmut Wieczorek and Prof. Felix Tiburcy (University of Osnabrück, Germany) for providing the V_1 antibody and Prof. Andrew Donini (York University, Canada) for providing the *A. aegypti* AQP1 antibody that were used in this study. We are also grateful to Prof. Ian Orchard (University of Toronto Mississauga, Canada) and Prof. Michael J. O'Donnell (McMaster University, Canada) for providing synthetic peptides, *Rhopr*DH and *Drome*DH_{31}, respectively, used in this study. We would like to thank the reviewers for their insightful comments and feedback which helped improve an earlier version of this manuscript. This research was funded by Natural Sciences and Engineering Research Council of Canada (NSERC) Discovery Grant (J.-P.V.P.), Ontario Ministry of Research Innovation Early Researcher Award (J.-P.V.P.), and NSERC CGS-D (F.S.) and the Carswell Scholarships in the Faculty of Science, York University (F.S.) along with a MITACS Globalink Research Internship (M.F.V.-M.).

Author affiliations: [a]Department of Biology, York University, Toronto, ON M3J 1P3, Canada; and [b]Departamento de Biología Celular y Fisiología, Instituto de Investigaciones Biomédicas, Universidad Nacional Autónoma de México, México City, 04510, México

1. K. W. Beyenbach, Transport mechanisms of diuresis in Malpighian tubules of insects. *J. Exp. Biol.* **206**, 3845–3856 (2003).
2. T. M. Clark, T. J. Bradley, Malpighian tubules of larval *Aedes aegypti* are hormonally stimulated by 5-hydroxytryptamine in response to increased salinity. *Arch. Insect Biochem. Physiol.* **34**, 123–141 (1997).
3. G. M. Coast, C. S. Garside, Neuropeptide control of fluid balance in insects. *Ann. N.Y. Acad. Sci.* **1040**, 1–8 (2005).
4. F. Sajadi, C. Curcuruto, A. Al Dhaheri, J.-P.V. Paluzzi, Anti-diuretic action of a CAPA neuropeptide against a subset of diuretic hormones in the disease vector, *Aedes aegypti*. *J. Exp. Biol.* **221**, jeb177089 (2018).
5. H. L. Lu, C. Kersch, P. V. Pietrantonio, The kinin receptor is expressed in the Malpighian tubule stellate cells in the mosquito *Aedes aegypti* (L.): A new model needed to explain ion transport? *Insect Biochem. Mol. Biol.* **41**, 135–140 (2011).
6. F. Sajadi *et al.*, CAPA neuropeptides and their receptor form an anti-diuretic hormone signaling system in the human disease vector, *Aedes aegypti*. *Sci. Rep.* **10**, 1755 (2020).
7. A. Ionescu, A. Donini, *Aedes*CAPA-PVK-1 displays diuretic and dose dependent antidiuretic potential in the larval mosquito *Aedes aegypti* (Liverpool). *J. Insect Physiol.* **58**, 1299–1306 (2012).
8. R. Jurenka, The PRXamide neuropeptide signalling system: Conserved in animals. *Adv. Insect. Phys.* (Academic Press, 2015), pp. 123–170.
9. S. A. Davies *et al.*, Signaling by *Drosophila* capa neuropeptides. *Gen. Comp. Endocrinol.* **188**, 60–66 (2012).
10. S. Terhzaz *et al.*, Mechanism and function of *Drosophila* capa GPCR: A desiccation stress-responsive receptor with functional homology to human neuromedinu receptor. *PLoS One* **7**, e29897 (2012).
11. H. A. MacMillan *et al.*, Anti-diuretic activity of a CAPA neuropeptide can compromise *Drosophila* chill tolerance. *J. Exp. Biol.* **221**, jeb185884 (2018).
12. A. R. Rodan, M. Baum, C. L. Huang, The *Drosophila* NKCC Ncc69 is required for normal renal tubule function. *Am. J. Physiol. Cell Physiol.* **303**, C883–C894 (2012).
13. X. H. Weng, M. Huss, H. Wieczorek, K. W. Beyenbach, The V-type H^+-ATPase in Malpighian tubules of *Aedes aegypti*: Localization and activity. *J. Exp. Biol.* **206**, 2211–2219 (2003).
14. H. Wieczorek, K. W. Beyenbach, M. Huss, O. Vitavska, Vacuolar-type proton pumps in insect epithelia. *J. Exp. Biol.* **212**, 1611–1619 (2009).
15. H. Wieczorek, The insect V-ATPase, a plasma membrane proton pump energizing secondary active transport: Molecular analysis of electrogenic potassium transport in the tobacco hornworm midgut. *J. Exp. Biol.* **172**, 335–343 (1992).
16. H. Wieczorek, M. Putzenlechnere, U. Klein, A Vacuolar-type proton pump energizes K^+/H^+ antiport in an animal plasma membrane. *J. Biol. Chem.* **266**, 15340–15347 (1991).
17. W. R. Harvey, S. H. P. Maddrell, W. H. Telfer, H. Wieczorek, H^+ V-ATPases energize animal plasma membranes for secretion and absorption of ions and fluids. *Am. Zool.* **38**, 426–441 (1998).
18. Y. Li *et al.*, RNA-Seq comparison of larval and adult malpighian tubules of the yellow fever mosquito *Aedes aegypti* reveals life stage-specific changes in renal function. *Front. Physiol.* **8**, 1–13 (2017).
19. M. L. Patrick, K. Aimanova, H. R. Sanders, S. S. Gill, P-type Na^+/K^+-ATPase and V-type H^+-ATPase expression patterns in the osmoregulatory organs of larval and adult mosquito *Aedes aegypti*. *J. Exp. Biol.* **209**, 4638–4651 (2006).
20. K. W. Beyenbach, T. L. Pannabecker, W. Nagel, Central role of the apical membrane H^+-ATPase in electrogenesis and epithelial transport in Malpighian tubules. *J. Exp. Biol.* **203**, 1459–1468 (2000).
21. R. M. Hine *et al.*, The excretion of NaCl and KCl loads in mosquitoes. *Am. J. Physiol. - Regul. Integr. Comp. Physiol.* **307**, R837–R849 (2014).
22. P. Dames *et al.*, cAMP regulates plasma membrane vacuolar-type H^+-ATPase assembly and activity in blowfly salivary glands. *Proc. Natl. Acad. Sci. U.S.A.* **103**, 3926–3931 (2006).

23. G. M. Coast, C. S. Garside, S. G. Webster, K. M. Schegg, D. A. Schooley, Mosquito natriuretic peptide identified as a calcitonin-like diuretic hormone in *Anopheles gambiae* (Giles). *J. Exp. Biol.* **208**, 3281–3291 (2005).
24. K. Karas, P. Brauer, D. Petzel, Actin redistribution in mosquito Malpighian tubules after a blood meal and cyclic AMP stimulation. *J. Insect Physiol.* **51**, 1041–1054 (2005).
25. C. Cady, H. H. Hagedorn, Effects of putative diuretic factors on intracellular second messenger levels in the Malpighian tubules of *Aedes aegypti*. *J. Insect Physiol.* **45**, 327–337 (1999).
26. D. H. Petzel, P. T. Pirotte, E. Van Kerkhove, Intracellular and luminal pH measurements of Malpighian tubules of the mosquito *Aedes aegypti*: The effects of cAMP. *J. Insect Physiol.* **45**, 973–982 (1999).
27. T. M. Clark, T. K. Hayes, K. W. Beyenbach, Dose-dependent effects of CRF-like diuretic peptide on transcellular and paracellular transport pathways. *Am. J. Physiol. - Ren. Physiol.* **274** (1998).
28. K. W. Beyenbach, H. Wieczorek, The V-type H^+ ATPase: Molecular structure and function, physiological roles and regulation *J. Exp. Biol.* **209**, 577–589 (2006).
29. F. J. S. Novak *et al.*, Primary structure of V-ATPase subunit B from *Manduca sexta midgut*. *BBA - Gene Struct. Expr.* **1132**, 67–71 (1992).
30. Y. X. Pan, H. H. Gu, J. Xu, G. E. Dean, *Saccharomyces cerevisiae* expression of exogenous vacuolar ATPase subunits B. *BBA - Biomembr.* **1151**, 175–185 (1993).
31. H. Wieczorek, D. Brown, S. Grinstein, J. Ehrenfeld, W. R. Harvey, Animal plasma membrane energization by proton-motive V-ATPases. *BioEssays* **21**, 637–648 (1999).
32. J. Zhang, Y. Feng, M. Forgac, Proton conduction and bafilomycin binding by the V0 domain of the coated vesicle V-ATPase. *J. Biol. Chem.* **269**, 23518–23523 (1994).
33. W. J. A. Dschida, B. J. Bowman, The vacuolar ATPase: Sulfite stabilization and the mechanism of nitrate inactivation. *J. Biol. Chem.* **270**, 1557–1563 (1995).
34. J. Rein, M. Voss, W. Blenau, B. Walz, O. Baumann, Hormone-induced assembly and activation of V-ATPase in blowfly salivary glands is mediated by protein kinase A. *Am. J. Physiol. - Cell Physiol.* **294**, C56–C65 (2008).
35. B. Zimmermann, P. Dames, B. Walz, O. Baumann, Distribution and serotonin-induced activation of vacuolar-type H^+-ATPase in the salivary glands of the blowfly *Calliphora vicina*. *J. Exp. Biol.* **206**, 1867–1876 (2003).
36. H. Wieczorek, G. Grüber, W. R. Harvey, M. Huss, H. Merzendorfer, The plasma membrane H^+-V-ATPase from tobacco hornworm midgut *J. Bioenerg. Biomembr.* **31**, 67–74 (1999).
37. P. Rosay *et al.*, Cell-type specific calcium signalling in a *Drosophila* epithelium. *J. Cell Sci.* **110**, 1683–1692 (1997).
38. M. C. Quinlan, N. J. Tublitz, M. J. O'Donnell, Anti-diuresis in the blood-feeding insect *Rhodnius prolixus* Stal: The peptide CAP(2b) and cyclic GMP inhibit Malpighian tubule fluid secretion. *J. Exp. Biol.* **200**, 2363–2367 (1997).
39. F. Tiburcy, K. W. Beyenbach, H. Wieczorek, Protein kinase A-dependent and -independent activation of the V-ATPase in Malpighian tubules of *Aedes aegypti*. *J. Exp. Biol.* **216**, 881–891 (2013).
40. K. W. Beyenbach, P. M. Piermarini, Transcellular and paracellular pathways of transepithelial fluid secretion in Malpighian (renal) tubules of the yellow fever mosquito *Aedes aegypti*. *Acta Physiol. (Oxf)* **202**, 387–407 (2011).
41. K. W. Beyenbach, Energizing epithelial transport with the vacuolar H^+-ATPase. *News Physiol. Sci.* **16**, 145–151 (2001).
42. T. Nishi, M. Forgac, The vacuolar (H^+)-ATPases – nature's most versatile proton pumps. *Nat. Rev. Mol. Cell Biol.* **3**, 94–103 (2002).
43. N. Nelson, W. R. Harvey, Vacuolar and plasma membrane proton-adenosinetriphosphatases. *Physiol. Rev.* **79**, 361–385 (1999).
44. K. W. Beyenbach, H. Skaer, J. A. T. Dow, The developmental, molecular, and transport biology of malpighian tubules. *Annu. Rev. Entomol.* **55**, 351–374 (2010).
45. P. M. Kane, Disassembly and reassembly of the yeast vacuolar H^+-ATPase in vivo. *J. Biol. Chem.* **270**, 17025–17032 (1995).
46. M. Voss, O. Vitavska, B. Walz, H. Wieczorek, O. Baumann, Stimulus-induced phosphorylation of vacuolar H^+-ATPase by protein kinase A. *J. Biol. Chem.* **282**, 33735–33742 (2007).
47. J. P. Sumner *et al.*, Regulation of plasma membrane V-ATPase activity by dissociation of peripheral subunits. *J. Biol. Chem.* **270**, 5649–5653 (1995).
48. G. Coast, The endocrine control of salt balance in insects. *Gen. Comp. Endocrinol.* **152**, 332–338 (2007).
49. M. J. O'Donnell, J. H. Spring, Modes of control of insect Malpighian tubules: Synergism, antagonism, cooperation and autonomous regulation. *J. Insect Physiol.* **46**, 107–117 (2000).
50. J. C. Williams, H. H. Hagedorn, K. W. Beyenbach, Dynamic changes in flow rate and composition of urine during the post-bloodmeal diuresis in *Aedes aegypti* (L.). *J. Comp. Physiol.* **153**, 257–265 (1983).
51. C. L. Jagge, P. V. Pietrantonio, Diuretic hormone 44 receptor in Malpighian tubules of the mosquito *Aedes aegypti*: Evidence for transcriptional regulation paralleling urination. *Insect Mol. Biol.* **17**, 413–426 (2008).
52. P. Gioino, B. G. Murray, J. P. Ianowski, Serotonin triggers cAMP and PKA-mediated intracellular calcium waves in Malpighian tubules of *Rhodnius prolixus*. *Am. J. Physiol. Regul. Integr. Comp. Physiol.* **307**, R828–R836 (2014).
53. F. Sajadi, J. P. V. Paluzzi, "Hormonal regulation and functional role of the 'renal' tubules in the disease vector, *Aedes aegypti*" in *Vitamins and Hormones*, G. Litwack, Ed. (Academic Press, 2021), pp. 189–225.
54. P. V. Pietrantonio, C. Jagge, C. McDowell, Cloning and expression analysis of a 5HT7-like serotonin receptor cDNA from mosquito *Aedes aegypti* female excretory and respiratory systems. *Insect Mol. Biol.* **10**, 357–369 (2001).
55. D. W. Lee, P. V. Pietrantonio, In vitro expression and pharmacology of the 5-HT7-like receptor present in the mosquito *Aedes aegypti* tracheolar cells and hindgut-associated nerves. *Insect Mol. Biol.* **12**, 561–569 (2003).
56. A. Petrova, D. F. Moffett, Comprehensive immunolocalization studies of a putative serotonin receptor from the alimentary canal of *Aedes aegypti* larvae suggest its diverse roles in digestion and homeostasis. *PLoS One* **11**, e0146587 (2016).
57. T. M. Clark, T. K. Hayes, G. M. Holman, K. W. Beyenbach, The concentration-dependence of CRF-like diuretic peptide: Mechanisms of action. *J. Exp. Biol.* **201**, 1753–1762 (1998).
58. D. H. Petzel, H. H. Hagedorn, K. W. Beyenbach, Preliminary isolation of mosquito natriuretic factor. *Am. J. Physiol. Regul. Integr. Comp. Physiol.* **18**, R379–R386 (1985).
59. J. A. Dow *et al.*, The Malpighian tubules of *Drosophila melanogaster*: A novel phenotype for studies of fluid secretion and its control. *J. Exp. Biol.* **197**, 421–428 (1994).
60. D. H. Petzel, M. M. Berg, K. W. Beyenbach, Hormone-controlled cAMP-mediated fluid secretion in yellow-fever mosquito. *Am. J. Physiol. Regul. Integr. Comp. Physiol.* **253**, R701–R711 (1987).
61. H. Kwon, H. L. Lu, M. T. Longnecker, P. V. Pietrantonio, Role in diuresis of a calcitonin receptor (GPRCAL1) expressed in a distal-proximal gradient in renal organs of the mosquito *Aedes aegypti* (L.). *PLoS One* **7**, e50374 (2012).
62. W. Kang'ethe, K. G. Aimanova, A. K. Pullikuth, S. S. Gill, NHE8 mediates amiloride-sensitive Na+/H+ exchange across mosquito Malpighian tubules and catalyzes Na+ and K+ transport in reconstituted proteoliposomes. *Am J. Physiol. Ren. Physiol.* **292**, 1501–1512 (2007).
63. A. K. Pullikuth, K. Aimanova, W. Kang'ethe, H. R. Sanders, S. S. Gill, Molecular characterization of sodium/proton exchanger 3 (NHE3) from the yellow fever vector, *Aedes aegypti*. *J. Exp. Biol.* **209**, 3529–3544 (2006).
64. P. M. Piermarini, D. Weihrauch, H. Meyer, M. Huss, K. W. Beyenbach, NHE8 is an intracellular cation/H^+ exchanger in renal tubules of the yellow fever mosquito *Aedes aegypti*. *Am. J. Physiol. Ren. Physiol.* **296**, 730–750 (2009).
65. H. Merzendorfer, M. Huss, R. Schmid, W. R. Harvey, H. Wieczorek, A novel insect V-ATPase subunit M9.7 is glycosylated extensively. *J. Biol. Chem.* **274**, 17372–17378 (1999).
66. M. C. Quinlan, M. J. O'Donnell, Anti-diuresis in the blood-feeding insect *Rhodnius prolixus* Stal: Antagonistic actions of cAMP and cGMP and the role of organic acid transport. *J. Insect Physiol.* **44**, 561–568 (1998).
67. S. Seino, T. Shibasaki, PKA-dependent and PKA-independent pathways for cAMP-regulated exocytosis. *Physiol. Rev.* **85**, 1303–1342 (2005).
68. M. Efetova *et al.*, Separate roles of PKA and EPAC in renal function unraveled by the optogenetic control of cAMP levels in vivo. *J. Cell Sci.* **126**, 778–788 (2013).
69. K. W. Beyenbach, A. Oviedo, D. J. Aneshansley, Malpighian tubules of *Aedes aegypti*: Five tubules, one function. *J. Insect Physiol.* **39**, 639–648 (1993).
70. J. A. Veenstra, Effects of 5-hydroxytryptamine on the Malpighian tubules of *Aedes aegypti*. *J. Insect Physiol.* **34**, 299–304 (1988).
71. J. P. V. Paluzzi, W. Naikkhwah, M. J. O'Donnell, Natriuresis and diuretic hormone synergism in *R. prolixus* upper Malpighian tubules is inhibited by the anti-diuretic hormone, *Rhopr*CAPA-α2. *J. Insect Physiol.* **58**, 534–542 (2012).
72. D. A. Rocco, D. H. Kim, J. P. V. Paluzzi, Immunohistochemical mapping and transcript expression of the GPA2/GPB5 receptor in tissues of the adult mosquito, *Aedes aegypti*. *Cell Tissue Res.* **369**, 313–330 (2017).
73. A. Lajevardi, F. Sajadi, A. Donini, J. P. V. Paluzzi, Studying the activity of neuropeptides and other regulators of the excretory system in the adult mosquito. *J. Vis. Exp.* **2021** (2021).
74. J. P. Ianowski, J. P. Paluzzi, V. A. Te Brugge, I. Orchard, The antidiuretic neurohormone *Rhopr*CAPA-2 downregulates fluid transport across the anterior midgut in the blood-feeding insect *Rhodnius prolixus*. *Am. J. Physiol. Integr. Comp. Physiol.* **298**, R548–R557 (2010).
75. M. Vanderveken, M. J. O'Donnell, Effects of diuretic hormone 31, *drosok*inin, and allatostatin A on transepithelial K^+ transport and contraction frequency in the midgut and hindgut of larval *Drosophila melanogaster*. *Arch. Insect Biochem. Physiol.* **85**, 76–93 (2014).
76. T. M. Clark, T. J. Bradley, Additive effects of 5-HT and diuretic peptide on *Aedes* malpighian tubule fluid secretion. *Comp. Biochem. Physiol. A Mol. Integr. Physiol.* **119**, 599–605 (1998).
77. V. Te Brugge, J. P. Paluzzi, D. A. Schooley, I. Orchard, Identification of the elusive peptidergic diuretic hormone in the blood-feeding bug *Rhodnius prolixus*: A CRF-related peptide. *J. Exp. Biol.* **214**, 371–381 (2011).
78. H. R. Lee, M. Zandawala, A. B. Lange, I. Orchard, Isolation and characterization of the corticotropin-releasing factor-related diuretic hormone receptor in *Rhodnius prolixus*. *Cell. Signal.* **28**, 1152–1162 (2016).
79. G. Overend *et al.*, A comprehensive transcriptomic view of renal function in the malaria vector, *Anopheles gambiae*. *Insect Biochem. Mol. Biol.* **67**, 47–58 (2015).
80. S. Jonusaite, S. P. Kelly, A. Donini, The physiological response of larval *Chironomus riparius* (Meigen) to abrupt brackish water exposure. *J. Comp. Physiol. B Biochem. Syst. Environ. Physiol.* **181**, 343–352 (2011).
81. S. D. McCormick, Methods for nonlethal gill biopsy and measurement of Na^+, K^+-ATPase activity. *Can. J. Fish. Aquat. Sci.* **50**, 656–658 (1993).
82. H. Chasiotis, S. P. Kelly, Occludin immunolocalization and protein expression in goldfish. *J. Exp. Biol.* **211**, 1524–1534 (2008).
83. F. Sajadi, M. F. Vergara-Martínez, J.-P. Paluzzi, The V-type H^+-ATPase is targeted in antidiuretic hormone control of the Malpighian "renal" tubules. Borealis. https://doi.org/10.5683/SP3/PADHU5. Deposited 17 November 2023.